Materials Physics and Mechanics. 2023;51(7): 124-136
Research article
http://dx.doi.org/10.18149/MPM.5172023_11

Submitted: August 7, 2023
Approved: September 20, 2023
Accepted: October 27, 2023

Physical and mechanical properties of modified chrome coatings

S. Vodopyanova ✉, G. Mingazova, R. Fomina, R. Sayfullin

Kazan National Research Technological University, Kazan, Russia

✉ vod-sveta@yandex.ru

Abstract. When solving the problems of improving the metal-surface treatment and giving special and anticorrosive properties to such surfaces, electrochemical composite coatings (ECCs) are essential. It is the dispersed phase that, being included in the metal matrix, gives the composite coatings a complex of new properties. This paper discusses how the aluminum/chromium oxide nanoparticles and high-dispersity graphite affect the physical and mechanical properties of coatings with a chrome matrix, i.e., corrosion resistance in 5 % NaCl, hardness, and wear resistance. Using the X-ray diffraction analysis, we have assessed how the particles under study affect the distribution of chromium over the surface of a steel sample. This paper also presents the microhardness test results for the heat treatment modes (temperature and time) of modified chrome coatings.

Keywords: electrochemical composite coatings; chrome matrix; the aluminum/chromium oxide nanoparticles; high-dispersion carbon; corrosion resistance; hardness; wear resistance; heat treatment

Citation: Vodopyanova S, Mingazova G, Fomina R, Sayfullin R. Physical and mechanical properties of modified chrome coatings. *Materials Physics and Mechanics*. 2023;51(7): 124-136. DOI: 10.18149/MPM.5172023_11.

Introduction

Currently, developing electrochemical composite coatings (ECCs) is an up-to-date sector of functional metal plating. Composite coatings are created where it is planned to obtain new properties, improve solidity or corrosion resistant characteristics, and enhance heat/scale resistance [1].

The principle of obtaining ECCs is based on the co-deposition of disperse particles (DPs) of various dispersion grades/nature and metals from the suspension electrolytes. Using various DPs in forming ECCs can help obtain modified strengthening coatings that encompass the properties, such as high corrosion resistance, corrosion protection in atmospheric conditions and in the environments affected by high temperatures and aggressive gases, and high wear resistance in abrasive conditions and in friction units [2].

Currently, some dozens of metals are used for ECCs [3–12]. Review article [13] organizes data on the metal-matrix-based composite coatings obtained over the years 2000-2019, depending on the metal nature and dispersion phase. Analysis of publications included in the VINITI Database RAS showed that producing composite plating coatings is one of the priority areas in the modern plating industry.

Among metal matrices used to obtain ECCs, we should distinguish the chrome one that has some valuable properties:

1. Chromium does not oxidize and does not change its color at temperature of up to 500 °C.
2. Chromium is resistant against most gases, acids, and alkalis.
3. High hardness of metallic chromium puts it on a par with corundum.

4. Chromium is of bluish-white color, similar to that of silver or platinum, which allows using it for decorative purposes.
5. In contrast to nickel, silver, or other metals, chromium is completely unaffected by the atmosphere and maintains its beautiful appearance.
6. Possibility to apply thick coatings firmly adhered to the base.

Of all electrodeposited metals, chromium has the least affinity for second-phase substances. Only in certain conditions, it is possible to obtain Cr-ECCs containing up to 2 % (mass) of dispersion phase [14].

This difficulty is associated with a low current efficiency of chromium (as little as 16-20 %), a significant hydrogen release, and formation of a cathode film preceding the metal release. This applies primarily to coatings obtained from suspension electrolytes containing electrically neutral particles that are highly resistant to electrolyte (Al_2O_3, TiO_2, ZrO_2). There have been a possibility of forming Cr-ECCs with some types of electroconductive particles, as well as the fact that the unsteady electrolysis factors can affect their formation. We also show the beneficial effects provided by organic compounds upon the co-deposition of DPs with chromium.

In [15], two dispersed phases were studied: A non-conductive one, BN (in the wurtzite modification) and an electrically conductive one, WC. We have assessed the physical and mechanical properties of the ECCs obtained, including the particles of wurtzite-BN, and noticed a considerable enhancement in both microhardness (increase of up to 38 %) and wear resistance (3-time decrease in wear-caused weight loss). It is found that the physical and mechanical properties of precipitations modified with WC particles, as well as their quality, are significantly inferior to chrome obtained from a standard chrome-plating electrolyte.

Ultrafine (nanometer-sized) particles are recognized as highly promising DP substances for creating efficient and functional ECCs, which allow improving the quality of the ECC performance characteristics and developing new-purpose materials, even with a lower DP content in the coating and the use of their low concentration in suspension electrolytes [16]. Widely using nano-sized particles is associated with the emergence of new substances, such as graphene, carbon nanotubes, nanodiamonds, silicon carbide, aluminum/silicon oxides, etc.

Authors of articles [17] and [18] have studied the properties of composite chrome-graphite coatings, i.e., chrome-containing multiwall carbon nanotubes (MWCNTs) obtained using particles of different dispersion. Graphite grades GC-3 (particles sized 40 ± 2 μm) and C1 (particles sized ~ 4 μm) and multiwalled carbon nanotubes were used as the dispersed phase. It is found that adding graphite of various grades to the chrome-plating solution leads to a slight decrease in roughness; that the graphite concentration in chrome-plating solution, while obtaining composite coatings, chrome-graphite does not practically affect the microhardness of the coatings; and that the total wear for the steel-ECC system (Cr–graphite GC-3) changes slightly, a decrease being observed in the graphite concentrations in the solution from 5 to 20 g/l. For the steel-ECC system (Cr-graphite C1), the total wear does not change. However, in both cases, there is a decrease in wear at lapping-in.

DPs affect changes in the parameters of chrome coatings micro- and substructures and, therefore, changes in the physical and mechanical properties of coatings [19].

This study is aimed at investigating of how aluminum/chromium oxide nanoparticles and high-dispersity black carbon affect the Cr-ECC properties.

Materials and Methods

To apply Cr-ECC, a standard chrome-plating electrolyte was used, composed as follows, in g/dm^3: CrO 3-250 (2.5 M), H_2SO_4 2.5 (0.025 M). Coatings were applied to steel samples sized 2 × 3 cm. We used the following as the second-phase particles:

1. Al_2O_3 nanopowder: TU 1791-002-36280340-2005: $S_{sp} = 21$ m^2/g; the average particle size is 30 nm;

2. Cr_2O_3 nanopowder is a solid green refractory powder with the content of the main substance is 98.4 %, S_{sp} = 27.4 m^2/g, d_{avg} = 42.7 nm;
3. high-dispersion graphite, C_{total} = 99.9 %, S_{sp} = 110 m^2/g, and ρ = 3.51 g/cm^3.

Electrolysis mode: $t = 50 \pm 5$ and 60 ± 5 °C; cathodic current density = 30 A/dm^2, and electrolysis time = 1 h. Lead plates were used as anodes, and electrolysis was performed with constant stirring with a magnetic stirrer.

Current efficiency (CE) of metal was computed by Faraday law. Coating thicknesses were found using the gravimetric method in accordance with the Russian standard GOST 9.302-88. Chemical composition of layers in the Fe-Cr system and the coating thicknesses were found using an X-ray fluorescence (XRF) analyzer (X-STRATA 980). Microhardness of coatings was found using the PMT-3M microhardness meter in accordance with GOST 9.450-76. Surface morphology was investigated using microscope ALTAMI MET-15. Structures of control coatings were studied using electronic microscope REM-100U with the energy-dispersive analyzer EDAR.

Corrosion resistance was measured using potentiostat IRC-Pro. We pre-varnished the samples, leaving a 5 × 5 mm square in the center. After the varnish dries, we degreased, dried, and tested the samples. Then we dipped each sample in a 5 % NaCl solution and turned on the machine.

In practice, rate indicators are conventionally used to assess corrosion resistance: corrosion rate C ($g/m^2 \cdot h$), which characterizes the rate of loss of metal mass during testing and the corrosion penetration rate P (mm/year). For electrochemical corrosion, the current corrosion index (C_i) can be used.

Experiment and Discussion

Coatings modified with Al_2O_3 nanoparticles. Coatings were obtained with a dispersed phase of Al_2O_3 at different temperatures and concentrations. Increasing the electrolysis temperature contributes to increasing the current efficiency of chromium (passivation of anodes decreases), to increasing the electrical conductivity, to decreasing the amounts of chromium-hydrogen penetrating in the electrolytic deposits, and to forming large-crystalline precipitates. The outcomes are presented in Table 1 below.

Table 1. Properties of chrome coatings depending on the concentration of Al_2O_3 nanoparticles in electrolyte and on the temperature

Electrolysis temperature, °C	50			60	
Concentration of particles in electrolyte, g/l	0	5	10	0	10
Coating thickness, μm	16	18	19.5	16.5	22
Deposition rate, μm/s	0.23	0.3	0.33	0.28	0.37
Current efficiency (CE) of metal, %	12	13.6	15	16.4	18

Introducing the Al_2O_3 nanoparticles into the electrolyte leads to forming more smoothed deposits with a greater thickness. In presence of nanoparticles, deposition rate and coating thickness increase. The greatest thickness and current efficiency of metal are observed in coatings obtained from the deposition electrolyte at the Al_2O_3 concentration of 10 g/l and at a temperature of 60 °C.

Table 2. Corrosion currents of the coatings ($Ki \cdot 10^4$, A/m^2)

Al_2O_3 concentration in electrolyte, g/l	Temperature, °C	
	50	60
0	7.9	7.9
5	11.06	12.68
10	–	13.83

We assessed the corrosion behavior of modified coatings by corroding current. Table 2 shows the results of identifying these indicators.

Corrosion penetration was computed by the following formula:

$$P = 8.76 \cdot Ki \cdot g, \quad (1)$$

where g is the metal density, g/cm^3 (chrome density, g = 7.1 g/cm^3).

Computation results are shown in Table 3.

Table 3. Corrosion penetration of chrome coatings, obtained from the suspension electrolyte

Concentration of Al_2O_3 particles in electrolyte, g/l	Corrosion penetration, mm/y	Score	Resistance group.
0(50)	0.001	1	Absolutely resistant
0(60)	0.001	1	Absolutely resistant
5(50)	0.0013	1	Absolutely resistant
10(50)	0.002	2	Very resistant
10(60)	0.002	2	Very resistant

Chromium is considered one of the most corrosion-resistant metals and used in protective coatings. The results obtained confirm that the optimal conditions for obtaining corrosion-resistant coatings are the particle concentration of 10 g/l and the temperature of 60 °C. The coatings have a smoothed surface and are of bluish color.

Al_2O_3 nanoparticles affect the mechanical properties of deposited coatings, resulting from changes in the electrochemical parameters of the electrode process, including the state of the surface films of hydroxide layers, and not as a result of the particles penetrating in the growing chrome layers [20].

The most important characteristic of coatings that protect metal is their continuity. Defective coatings are less corrosion-resistant. Surfaces of the samples obtained were examined microscopically. Surfaces of control samples are uniform, with small cracks. However, the surfaces of the modified coatings have large and long cracks, which affects their corrosion resistance, reducing it. Since corrosion processes start on open surfaces and the metal destruction is accompanied by the appearance of an electric current flowing between the anode and cathode sections of the metal, the Cr-Al_2O_3 structure will contribute to spreading the corrosion into the depth of the coating due to cracks.

As active cathodic inclusions, the Al_2O_3 particles can cause, reducing the corrosion resistance. Particles are involved in various redox processes occurring on the coating surface.

Coatings modified with Cr_2O_3 nanoparticles. The coatings were obtained from an electrolyte with the DPs of Cr_2O_3 at the concentrations ranging from 10 to 50 g/l. Electrolysis temperature 50 °C. During visual inspection, we found that the samples obtained from the electrolyte with the DP concentration of 10 g/l had a silvery luster, and they were light.

Samples obtained from the deposition electrolyte with the particles concentration of 20 g/l have a noticeably smaller shine than that of the samples obtained from the 10 g/l electrolyte. Samples obtained from electrolyte with the concentrations of 30, 40, or 50 g/l do not shine, they are matte. With an increase of the DP concentrations in electrolyte, the color of samples was slightly darker. Figures 1-3 show the structures of modified coatings.

If follows from Fig. 1 that the galvanic chrome structure has large and deep cracks. Surface is uneven, there are dendrites in the form of well-formed globules with a diameter of 30-50 μm, consisting of needle-like elements. Oxygen content is 4.67 %, and chrome content is 95.36 %.

Figures 2 shows the structure of a modified coating at the Cr_2O_3 concentration of 10 g/l in the deposition electrolyte. Chromium particles are densely packed and faceted, sized 10-20 μm, microglobules (20-30 μm) are with small chromium particles (1-2 μm). Oxygen content is 4 %, and chrome content is 96 %. No cracks, and there are significantly fewer dendrites, as compared

to the control coating. Globule sizes are also smaller than those of the control coating. Metallic chromium is formed at active sites and at a closer distance from each other than in the control sample. It can be assumed that nanoparticles affect the cathode surface state and thus improve the electrode processes, activating more cathode sites at which chromium is reduced.

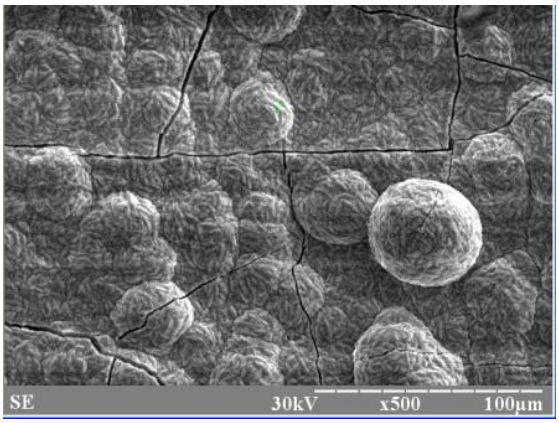

Fig. 1. Structure of control coating

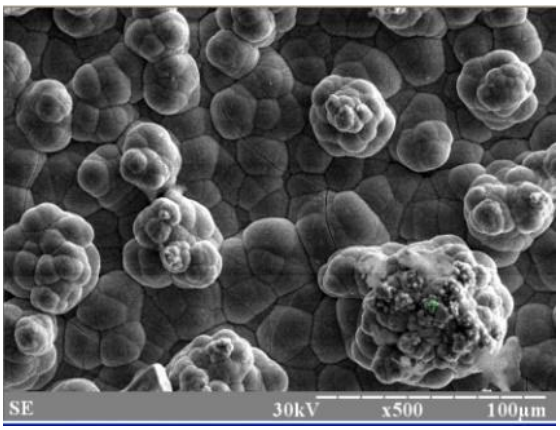

Fig. 2. Structure of the modified coating at a concentration of Cr_2O_3 in the electrolyte of 10 g/l

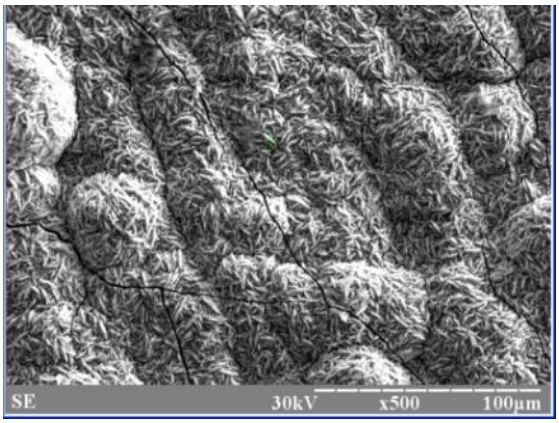

Fig. 3. Structure of the modified coating at a concentration of Cr_2O_3 in the electrolyte of 20 g/l

Figures 3 shows that the structure is represented by chromium microglobules sized ~ 10 µm. Oxygen content is 5 %, and chrome content is 95 %. Table 4 shows the results of identifying the main indicators of applying the modified coatings.

Table 4. Properties of chrome coatings depending on the concentration of the Cr_2O_3 nanoparticles in electrolyte

Concentration of particles in electrolyte, g/l	0	10	20	30	40	50
Coating thickness, µm	19.6	21.3	22.3	23.0	23.8	24.2
Deposition rate, µm/s	0.33	0.36	0.37	0.38	0.4	0.4
Current efficiency (CE) of metal, %	13.8	15	16.1	18.5	18.8	19.4

Slight increase in the thickness of samples obtained from the pure electrolyte is explained by the treeing taking place at the sample edges during electrolysis. Subsequently, removing them during mechanical treatment affects the weight gains of the coating and, therefore, the thickness computations.

In presence of DPs in electrolyte, treeing is observed to a lesser extent, while the deposition rate and coating thickness increase. At concentrations in the electrolyte of 30, 40, or 50 g/l, no treeing was observed at all.

As can be seen from the table, DPs of Cr_2O_3 provide a good effect on the current efficiency of chrome. CE value increases with the increase in the concentration of particles and reaches its maximum value of 19.4 % in electrolyte with the DP concentration of 50 g/l.

Non-destructive quality control and identifying the elemental composition of the samples were performed using the analyzer X-STRATA 980. To assess the control and composition of modified coatings, we identified the contents of chromium and iron [21].

To assess the uniformity of the chromium distribution over the sample surface, we performed measurements at three different points on the samples (top, middle, and bottom – points 1, 2, and 3, respectively). Our findings are shown in Table 5.

Table 5. Results of finding the percentage of chrome and iron contents, depending on the DPs concentration in electrolyte

DPs concentration in electrolyte	Points	Chrome content, %	Iron content, %
0	1	55.87	21.91
	2	68.99	8.31
	3	77.52	2.55
10	1	86.33	0.38
	2	88.94	0.43
	3	90.86	0.17
20	1	69.3	9.90
	2	77.55	4.52
	3	83.22	1.96
30	1	83.95	1.08
	2	86.21	0.66
	3	90.16	0.18
40	1	72.88	5.55
	2	83.59	1.72
	3	86.60	0.51
50	1	75.12	4.07
	2	79.45	2.2
	3	80.07	1.77

Based on Table 5, we can conclude that the most "nonuniform" samples were obtained from the control electrolyte. Coatings obtained from the suspension electrolyte are very uniform in terms of chromium content, with a high content and, therefore, high hardness and brittleness of chromium. Table 6 shows the results of identifying the hardness of coatings.

Table 6. Hardness of modified chrome coatings

DPs concentration in electrolyte	0	10	20	30	40	50
Hardness, GPa	7.75	11.8	11.1	9.2	9.6	9.6

DPs have a positive impact on the hardness of chrome ECCs. The best effect is provided by the DP concentration of 10 g/l: hardness increased to the highest value of 11.8 GPa.

We studied how the thermal treatment of modified chrome coatings affects microhardness.

We annealed the samples obtained from the control electrolyte and from the electrolyte with DPs of Cr_2O_3, 10 mg/l. Annealing was carried out at temperatures of 300, 600, and 900 °C and at the annealing duration of 1 and 2 h. Upon annealing, we identified the values of microhardness. Table 7 shows the results of identifying the hardness of the annealed samples.

Table 7. Hardness of the annealed modified coating samples

Annealing temperature, °C	300		600		900	
Annealing duration, h	1	2	1	2	1	2
Without DPs	9.1	7.3	7.1	12.0	4.8	2.5
DPs, 10 g/l	9.6	10	10.3	12.4	5.1	3.7

At 300 °C, the appearance of samples has not changed, and there are no cracks. Metal chrome had a good appearance. At 600 °C, the color of the samples changed from light gray to bright blue, the samples obtained from the electrolyte with the additive having a brighter color and being more uniform. Samples that had been annealed for just 1 h were of pale blue color. Neither pure chromium nor its oxides can be blue. Chromium salts are of sky-blue color. Chromium (III) chloride, $CrCl_3$, represents purple crystals. It is soluble in water in the presence of reducing agents (Cr^{2+}, Fe^{2+}). It is used in obtaining chromium by electrolysis and by metallothermic process. At 900 °C, with the annealing lasting for 1 hour, the samples become dark green. Samples obtained from the control electrolyte had large cracks and were destructed at some points. Samples obtained from electrolyte with DPs have no cracks and have not been damaged. If annealing lasted 2 h, the samples were black, crack-free, and strong.

Coatings modified with high-dispersion carbon. To identify the optimal parameters of obtaining composite coatings, we studied how the concentration of high-dispersion particles of black carbon affected the properties of Cr-ECC. Table 8 shows the results of finding the basic parameters of the electrochemical reduction of chrome from the suspension electrolyte.

Table 8. Properties of chrome coatings depending on the concentration of high-dispersion graphite particles in electrolyte

Concentration of particles in electrolyte, g/l	0	5	10	15	20
Deposition rate, μm/h	10.56	11.69	15.27	17.86	20.11
Current efficiency (CE) of metal, %	9.54	10.2	11.01	12.87	14.49
Hardness (H), GPa	7.7	9.23	10.11	9.67	9.11

In all the experiments, coatings were matte and silver-gray. It follows from Table 8 that, with increasing the concentration of graphite particles, the deposition rate of coatings increases. With an increase in DP concentration, the current efficiency of chromium increases from 10 to 15 %. The highest CE value is reached at the concentration of 20 g/l.

Graphite particles contribute to increasing the hardness at smaller concentrations only. If the concentrations in deposition electrolyte is higher, 15 and 20 g/l, then the hardness of samples decreases. The highest hardness value, 10 GPa, can be reached at the concentration of 10 g/l.

It is characteristic of most ECCs that the increase in hardness is determined by changing the matrix structure, grinding the grains, increasing the displacement resistance of individual components of the system with the existing particles, and finally by the presence of the second-phase substances that have a much higher hardness than the matrix.

Decreasing ECC hardness can be found, where materials having lower density are used, such as graphite, disulfide, or molybdenum. This is due to the fact that, when contacting the anode, these particles, in most cases, don't have a sufficient force pulse to ensure a tight contact, and in some cases, they penetrate in the coating as agglomerated groups that give the coating a reduced porosity. With a smaller ECC thickness, the hardness is found for the coating and its sublayer.

To identify the chemical composition of the chrome layers, we used X-ray diffraction analysis. Top, middle, and bottom of the sample were selected as the measurement points of chrome distribution over the metal. The outcomes are presented in Table 9 below. Results shown in Table 9 confirm the outcomes shown in Table 8 above. Since the system under study is a single-layer one, it is natural that the greater the coating thickness, the higher the chromium content.

Table 9. Identifying the chemical composition of chrome layers, %

Concentration, g/l		0	5	10	15	20
"Top"	Cr	41.53	62.85	65.7	68.75	87
	Fe	44.77	13.35	21.5	9.95	0.9
"Middle"	Cr	82.88	83.5	85.05	86.83	96.1
	Fe	0.76	0.45	0.5	0.52	0.7
"Bottom"	Cr	92.47	93.45	96.9	99.1	99.8
	Fe	0.34	0.45	0	0.13	0.11

In control samples, chromium is distributed over the surface of the metallic sample non-uniformly. Chromium is mostly deposited in the middle and bottom of the samples. This can be explained by the poor throwing power of chrome electrolyte. When introducing in the electrolyte the graphite particles at their concentration of 5-15 g/l, chrome content in the coating increases, the influence of particles being observed to a larger extent in the "tops" of the samples. The thickness of the "bottom" changes slightly in all the coatings.

It can be concluded that graphite provides good effects on the throwing power of chrome electrolyte. More uniform, in terms of their compositions, were coatings obtained at the 20 g/l concentration of ultrafine graphite particles. The findings are consistent with the results of computing the CEs (Table 8).

Heat treatment is performed to relieve internal stresses, increase the plasticity of deposits, and homogenize the coating structure. When performing the heat treatment of a dispersed-phase substance can either be partly removed from the superficial layer or be modified and thereby affect the coating structure.

Hydrogen content can be reduced by annealing. Annealing had been performed at a temperature of 300, 600, and 900 °C in an electric furnace until a constant coating mass was established. During annealing, the coating masses decreased by thousandths of a gram. We investigated the influence of graphite particles on the hydrogen content in the chrome matrix. As a criterion for evaluating the hydrogen effect, we took weight before and after annealing and measured the coating hardness.

Hardness was evaluated in control samples after annealing at all the temperatures studied. Hardness of modified coatings was evaluated after annealing them at the temperature of 600 °C. The results are shown in Table 10.

Table 10. Hardness of coatings depending on the annealing temperature

Concentration of particles, g/l	Temperature, °C		
	300.00	600.00	900.00
	Hardness, H, GPa		
0	7.70	8.00	8.90
	Time, h		
	1.00	2.00	1.00
5	10.74		
	1.00		
10	11.03		
	2.00		
15	11.64		

Table 10 shows that the hardness of the coatings after annealing increased by an average of 2.7 GPa in coatings at the 5 g/l concentration of particles in electrolyte. Appearance of the coatings: at a temperature of 300 °C, thin films were formed on the samples, which were not at all noticeable to the eye.

At 600 °C, violet-blue films were formed on the smooth surface of metal as a result of forming a thin transparent surficial oxide film and of the light interference in it. Color was

affected by the rate of temperature elevation (from 300 up to 600 °C) and by the holding time (2 hours) of metal samples at such temperature.

These iridescent colors can be observed on the shiny surface of steel objects heated; and they are called "annealing colors". These colors develop due to the fact that, resulting from heating the steel to high temperatures, its surface gets oxidized to form a thin transparent oxide film that reflects light in different ways depending on its thickness, which makes us see one or another annealing color. At the points where the heating temperature was higher, the oxide film thickness is greater, respectively, because at higher temperatures the diffusion rate is higher and the oxygen atoms penetrate deeper; thicker oxide films absorb light waves with a longer wavelength and reflect those with a smaller one.

There is a direct relationship between the film thickness and the wavelength of the light reflected by it: The greater the film thickness is, the shorter-wave reflected light we get. For example, blue is formed when longer waves are "subtracted" from the white, such as red or orange, while yellow is formed when short-wave radiation, such as violet or blue, is "subtracted" from the spectrum. Therefore, blue color is relevant to a higher heating temperature, while yellow color to a lower one.

Many factors influence on the annealing steel color formation: Heating rate, holding time, and steel composition. For example, in alloyed steels (especially with chromium), oxide films are formed slower and at higher temperatures than in common carbon steels.

The oxide film is of such a color due to the fact that hexavalent chromium is oxidized to the trivalent one when heated. As is known from literary references, trivalent chromium salts have a violet and a green modification, the salts of such modifications having different structures.

At 900 °C, well-visible thick marsh-green films were formed; this color is due to forming the trivalent chromium oxide film that a typical green color.

Heating improves the adhesion of chrome coatings to metal, but the heating should not exceed 600 °C, because at the same time, a brittle carbide layer is formed at the boundary between steel and chromium, along which the samples are exfoliated if deformed.

During the thermal oxidation of metallic chromium, chromium (III) oxide can be formed in the coating, as well as chromium hydrides and carbides. Chromium hydride is not formed, since about 80 % of hydrogen is released at 300 °C and the remaining 20 % only at higher temperatures, while chromium recrystallization starts at 900 °C.

Heating improves the adhesion of chrome coatings to metal, but the heating should not exceed 600 °C, because at the same time, a brittle carbide layer is formed at the boundary between steel and chromium, along which the samples are exfoliated if deformed.

Figures 4-10 show the microstructures of coatings, depending on the annealing conditions and the graphite concentrations in the electrolyte.

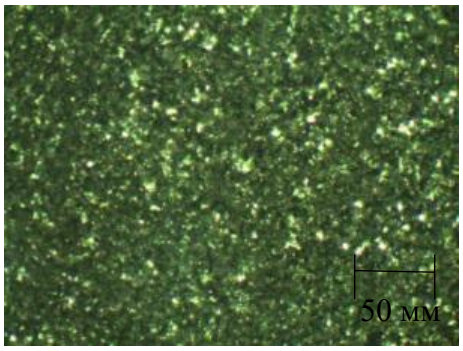

Fig. 4. Control coating microstructure before burning

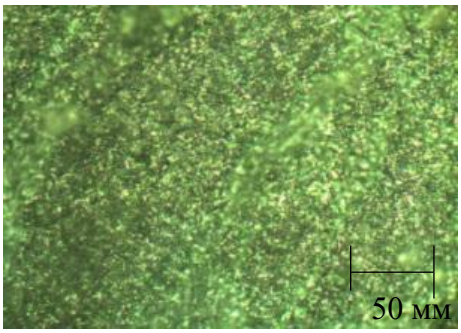

Fig. 5. Control coating microstructure after annealing at 300 °C

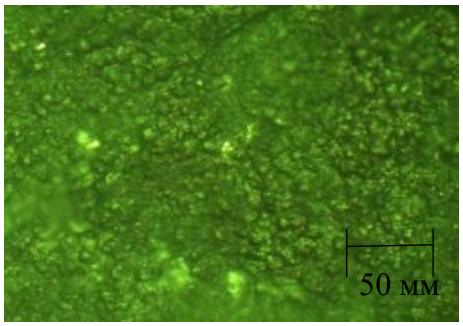

Fig. 6. Control coating microstructure after annealing at 600 °C

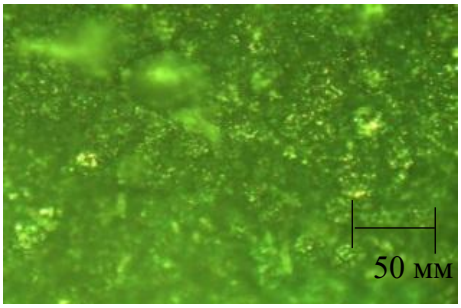

Fig. 7. Control coating microstructure after annealing at 900 °C

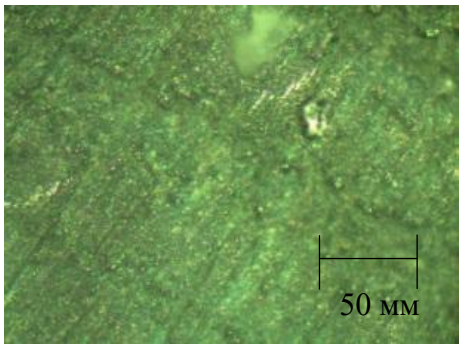

(a)

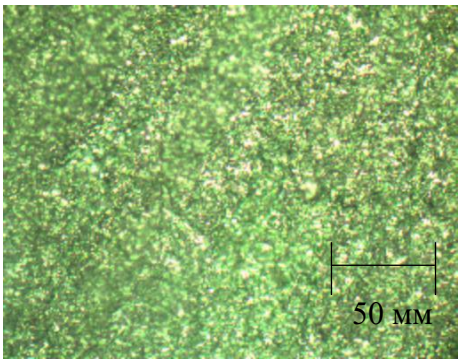

(b)

Fig. 8. Chrome coating microstructure at the graphite concentration of 5 g/l in electrolyte (a) before and (a) after annealing at 300 °C

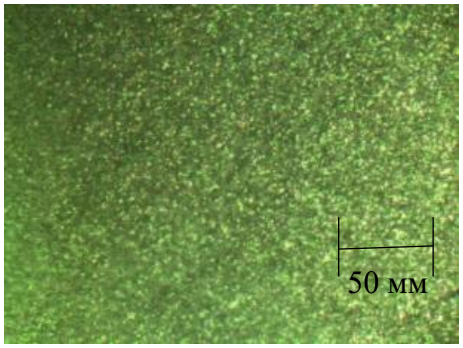

(a)

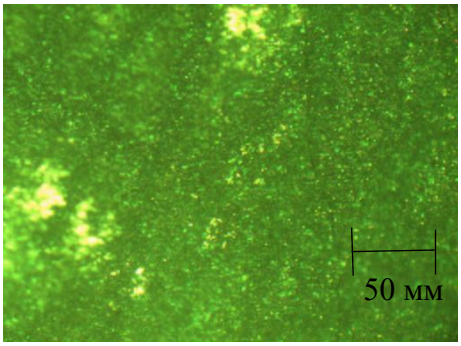

(b)

Fig. 9. Chrome coating microstructure at the graphite concentration of 10 g/l in electrolyte (a) before and (b) after annealing at 600 °C

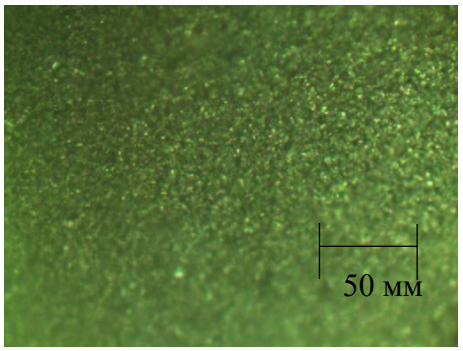

(a)

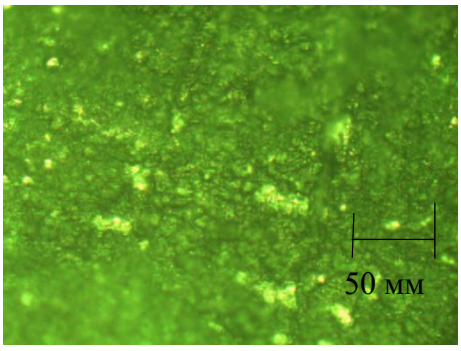

(b)

Fig. 10. Chrome coating microstructure at the graphite concentration of 15 g/l in electrolyte (a) before and (b) after annealing at 900 °C

Microphotographs show that chrome coatings have different structures. With the transition of no-DP chrome coating to the ECC, the surface microstructure changes significantly. The surface is better developed and has a noticeable shine; it also has darker areas, corresponding to possible inclusions of graphite particles in the chrome matrix.

Total corrosion rate is evaluated by losing the metal per unit area of corrosion, e.g., in $g/m^2 \cdot h$, or by the corrosion penetration rate, i.e., by a single side decrease in the intact metal thickness (P), e.g., mm/year. Tables 11 and 12 present the results of evaluating the corrosion resistance of modified coatings.

Table 11. Influence of annealing conditions on the gas corrosion rate

Annealing temperature, °C	Concentration of particles, g/l	V gas corrosion rate, g/m^2*h			
300	0	$1.1 \cdot 10^{-4}$	$3.83 \cdot 10^{-6}$	$4.8 \cdot 10^{-4}$	$3.3 \cdot 10^{-6}$
	5				
600	0	$1.77 \cdot 10^{-6}$	$3.33 \cdot 10^{-4}$	$3.77 \cdot 10^{-5}$	$2.44 \cdot 10^{-3}$
	10				
900	0	$1.15 \cdot 10^{-6}$	$1.7 \cdot 10^{-12}$	$2.95 \cdot 10^{-9}$	$2.25 \cdot 10^{-10}$
	15				

Table 12. Corrosion penetration of modified coatings

Temperature, °C	Concentration of particles, g/l	Corrosion penetration, mm/year			
300	0	0.03	0.05	0.07	0.06
	5				
600	0	0.454	0.21	0.58	0.47
	10				
900	0	0.008	0.002	0.005	0.097
	15				

Gas corrosion rate increases greatly with the temperature exceeding 200-300 °C. The samples of control coatings turned out to be resistant, if they had been annealed at 300 °C and with particles at a concentration of 5 g/l in the deposition electrolyte and at 600 °C with particles of 10 g/l. Samples annealed at 900 °C and the concentration of 15 g/l turned out to be less resistant. Corrosion resistance of coatings is due to forming a protective film, Cr_2O_3, on the surface. Thickness and composition of this film are evaluated by the coating surface state and by the conditions of evaluating the corrosion resistance. Table 13 shows the results of evaluating the average wear of samples.

Table 13. Average wear of the samples obtained from electrolytes of different compositions.

Electrolyte composition	Average wear, mg
Control coating	0.0216
Standard electrolyte with 5 g/l of graphite	0.0289
Standard electrolyte with 10 g/l of graphite	0.0189
Standard electrolyte with 15 g/l of graphite	0.0295

As can be seen from Table 13, the sample obtained from a standard electrolyte with 10 g/l of ultrafine graphite particles demonstrates the least wear, and the dispersed-phase coating resists the wear 1.1 times better than galvanic chromium deposits.

Conclusion

Changes in the physical and mechanical properties of chrome matrix are caused by the effect of dispersed-phase particles, such as aluminum/chromium oxide nanoparticles and high-dispersion carbon, on the state of the deposited chrome layers. When introducing the dispersed phase into the electrolyte, the surface of the electrically deposited chrome gets smoothed, and thicker coatings are obtained. Using the XRF method, we have shown that introducing DPs in the electrolyte contributes to a more uniform chrome distribution over the entire surface of steel samples.

With changes in the concentration of the Cr_2O_3 particles in electrolyte from 10 to 50 g/l, the hardness of deposits increases by 1.2-1.5 times, while when using high-dispersion graphite particles of 5-20 g/l, this indicator changes by 1.2–1.3 times.

In studying corrosion currents, we found that coatings obtained from electrolytes with the Al_2O_3 nanoparticles had corrosion currents greater than those of coatings from a standard chrome-plating electrolyte. Moreover, with an increase in the DP content, the corrosion current increases.

References

1. Sayfullin RS. *Composite coatings and materials*. Moscow: Khimiya; 1977. (In-Russian)
2. Yudina EM, Kisel YE, Kadyrov MR, Serguntsov AS. Service properties of composite electrochemical coating. *MATEC Web Conf.* 2021;344: 01022.
3. Vodopyanova SV, Fomina RE, Mingazova GG. Properties of Composite Electrochemical Coatings with a Nickel Matrix. *Bulletin of Kazan Techn ol. Un-ty*. 2011;11: 156–160.
4. Dolmatov VY, Burkat GK, Safronova IV, Vehanen A, Myllymäki V, Marchukov VA, Almazova NS, Litovka YV, Dyakov IA. The Study of Obtaining Composite Nickel Electroplatings with Detonation Nanodiamonds and Diamond Charge. *Advanced Materials and Technologies*. 2020;20(4): 3–11.
5. AlOgab KA, Borisevich IO, Borisevich KO, Zhdanok SA, Krauklis AV, Parshuto AA. Preparation of chromium coatings with additions of carbon nanotubes. *Protection of Metals and Physical Chemistry of Surfaces*. 2018;54(3): 360–364.
6. Tseluikin VN. Preparation and properties of graphite nitrate-modified composite electrochemical coatings based on a nickel–chromium alloy. *Inorganic Materials*. 2019;55(7): 656–658.
7. Tseluikin VN, Yakovlev AV. Study of electrodeposition and functional properties of nickel–graphite bisulfate composite coatings. *Russian Journal of Applied Chemistry*. 2019;92(5): 614–619.
8. Tseluikin VN, Yakovlev AV. On the electrochemical deposition and properties of nickel-based composite coatings. *Protection of Metals and Physical Chemistry of Surfaces*. 2020;56(2): 374–378.
9. Bratkov IV, Yudina TF, Melnikov AG Bratkov AV. Production and properties of electrochemical coatings with electrochemically dispersed graphene based on nickel matrix. *ChemChemTech.* 2020;63(8): 90–95. (In-Russian)
10. Vinokurov EG, Margolin LN, Farafonov VV. Elecrtodeposition of composite coatings. *ChemChemTech.* 2020;63(8): 4–38. (In-Russian)
11. Tseluikin VN, Dzhumieva AS, Yakovlev AV, Mostovoy AS. Electrochemical deposition and properties of nickel–chromium–grapheme oxide composite coatings. *Protection of Metals and Physical Chemistry of Surfaces*. 2021;57(6): 1231–1234.
12. Pyanko AV, Alisienok OA, Kubrak PB, Chernik AA. Formation and physicochemical properties of composite electrochemical coatings of TiN–Nickel alloy with silicon dioxide incapsulated by nanosized titanium dioxide. *Russian Journal of Electrochemistry*. 2022;58(5): 418–424.
13. Vinokurov EG, Margolin LN, Farafonov VV. Electrodeposition of Composite Coatings. *News of Higher Educational Institutions. Chemistry and Chemical Engineering*. 2020;63(8): 4–38.

14. Belenky MA, Ivanov AF. *Electrodeposition of metal coatings*. Moscow: Metallurgiya; 1985. (In-Russian)
15. Zheleznov EV, Kuznetsov VV. Chromium-based Composite Coatings Deposited from Cr (VI) Baths Containing Ultradispersed Particles of BNWuerzie and WC. *Electroplating and processing Surfaces*. 2017;1: 34–40. (In-Russian)
16. Sayfullin RS, Khatsrinov AI, Vodopyanova SV, Fomina RE, Mingazova GG. Research in the field of creating composite electrochemical coatings (ECC) with a dispersed phase of micro- and nanoparticles. *Bulletin of Kazan Technol. Un-ty*. 2009;6: 80–91.
17. Makhina VS, Grafushin RV, Vinokurov EG. Wear Resistance of Composite Electrodeposited Coatings Chrome-Graphite. *Advances in Chemistry and Chem. Eng.* 2017;31(5): 54–56.
18. Grafushin RV, Vinokurov EG, Makhina VS, Burukhina TF. Electrodeposition and physic-mechanical properties of composite coatings based on chrome with various carbon modifications. *Electroplating and Processing Surfaces*. 2018;26(2): 26–32. (In-Russian)
19. Korneychuk NI. Influence of heat treatment conditions on the structure of chrome coatings *Engineering. Information Science*. 2015;51(3): 90–96.
20 Lubnin EN, Polyakov NA, Polukarov YM. Electrodeposition of Chromium from Sulfate-Oxalate Solutions Containing Aluminum Oxide and Silicon Carbide Nanoparticles. *Metal Protection*. 2007;43(2):199–206.
21. Vodopyanova SV, Sayfullin RS, Fomina RE, Mingazova GG. Evaluation of the thickness and chemical composition of chromium coatings with Cr_2O_3 nanoparticles. *Bulletin of Kazan Technol. Un-ty*. 2015;18(4): 125–128.